Food Chemistry: Molecular Sciences 10 (2025) 100232

Contents lists available at ScienceDirect

Food Chemistry: Molecular Sciences

journal homepage: www.sciencedirect.com/journal/food-chemistry-molecular-sciences

Integrated transcriptomic and proteomic analyses provide insights into the biosynthesis of Lycii fructus polysaccharides from different cultivation regions

Limei Tong [a], Yinxiu Jiang [a], Xinrun Zhang [a], Xia Zhang [b,*], Yihao Zheng [a,c], Qiheng Zhao [a,d], Sheng Yu [a], Wenhua Zhang [e], Gang Ren [f], Zhanping Chen [f], Yuling Zhao [g], Sheng Guo [a], Hui Yan [a], Shulan Su [a], Yang Pan [a], Jin-ao Duan [a,*], Fang Zhang [a,*]

[a] Jiangsu Collaborative Innovation Center of Chinese Medicinal Resources Industrialization, School of Pharmacy, Nanjing University of Chinese Medicine, Nanjing 210023, PR China
[b] School of Pharmacy, Key Laboratory of Minority Medicine Modernization, Ministry of Education, Ningxia Medical University, Yinchuan 750021, PR China
[c] School of Global Public Health, New York University, New York, NY 10003, United States
[d] School of Chinese Materia Medica, Nanjing University of Chinese Medicine, Nanjing 210023, PR China
[e] Bairuiyuan Gouqi Co., Ltd, Yinchuan 750200, China
[f] Haixi Agriculture and Animal Husbandry Technology Extension Service Center, Delingha 817000, China
[g] Jinghe Gouqi Industry Development Center of Bortala Mongolian Autonomous Prefecture, Bortala 833399, China

ARTICLE INFO

Keywords:
Lycii fructus
Polysaccharides
Biosynthesis
Transcriptomic analysis
Proteomic analysis

ABSTRACT

Polysaccharides from L. fructus (LFPs) serve as important active biomacromolecules for the wide spectrum of bioactivities exhibited by Lycii fructus. However, the influence of ecological environments on the biosynthesis and structural characteristics of LFPs remains largely unexplored. The present research conducted a comprehensive strategy combining physicochemical structural elucidation, stoichiometric analysis, transcriptomic profiling, and proteomic analysis in L. fructus samples collected from typical cultivation regions including Ningxia, Xinjiang, and Qinghai. The results revealed distinct structural variations in LFPs from Ningxia compared to those from other regions in terms of Glc, Ara, GalA composition percentages as well as overall content. The omics data identified 5531 and 8084 differentially expressed genes (DEGs), as well as 3728 and 4732 differentially expressed proteins (DEPs) in Xinjiang and Qinghai compared to Ningxia, respectively. The integration of transcriptomic and proteomic analyses revealed enrichment of DEGs and DEPs involved in the biosynthesis pathway of LFPs, including UDPs, AXS, and UGDH. Temperature and precipitation were the significant ecological factors affecting LFPs biosynthesis. These comprehensive analyses provide a novel perspective for explaining the important material basis and environmental response mechanism underlying the quality formation of L. fructus.

1. Introduction

Polysaccharides represent the most diverse category of macromolecular polymeric structures in the biosphere. Nature-derived polysaccharides are undeniably among the most intriguing due to their various significant biological functionalities and activities, including antioxidant, antimicrobial, anticancer, anti-thrombotic, hypoglycemic, immunomodulatory, intestinal flora balancing properties, and senescence delay effects (Gericke et al., 2024). The application of polysaccharides has been considered a promising strategy for preventive or therapeutic use against a variety of human diseases.

Thereinto, nature plant polysaccharides are a kind of polysaccharides synthesized in plants, which not only exhibit interesting beneficial activities, but also play crucial roles in maintaining growth, development, cell wall integrity and imparting resistance in response to abiotic stressors such as salinity, mental pressure, and drought. The process of environmental adaptation leads to variations or disruptions in the expression levels of enzymes involved in carbohydrate synthesis,

* Corresponding authors.
E-mail addresses: 20210857@njucm.edu.cn (L. Tong), 20220807@njucm.edu.cn (Y. Jiang), 20230634@njucm.edu.cn (X. Zhang), zhangxia@nxmu.edu.cn (X. Zhang), yz8609@nyu.edu (Y. Zheng), zhaoqiheng323@zidd.ac.cn (Q. Zhao), yusheng@njucm.edu.cn (S. Yu), guosheng@njucm.edu.cn (S. Guo), yanhui@njucm.edu.cn (H. Yan), sushulan@njucm.edu.cn (S. Su), ypan@njucm.edu.cn (Y. Pan), dja@njucm.edu.cn (J.-a. Duan), fangzhang@njucm.edu.cn (F. Zhang).

https://doi.org/10.1016/j.fochms.2024.100232
Received 1 August 2024; Received in revised form 18 November 2024; Accepted 1 December 2024
Available online 5 December 2024

resulting in disparities in the content and molecular compositions of polysaccharides. For example, water treatment process resulted in higher concentrations of polysaccharides and uronic acid in *Allium roseum* leaves compared to those treated with alkali or chelate, while the monosaccharide composition remained unchanged. After treatment, the polysaccharide exhibited specific antioxidant activity (Teka et al., 2022). In another study conducted on *Ophiopogon japonicus* collected from regions with contrasting climates (Zhejiang province in eastern China vs Sichuan province in southwest China), variations were observed in the contents and molecular characteristics of polysaccharides between these two regions. *O. japonicus* from Zhejiang exhibited a higher fructose content compared to its counterpart from the Sichuan region, resulting in enhanced antioxidant properties and immune-boosting effects (Z. Chen et al., 2022). A recent study reported that despite having similar monosaccharide compositions, Alfalfa polysaccharide displayed ecologically sensitive molar ratios between arabinose and galacturonic acid under saline-alkali conditions present in soil (Zhang, Kim, et al., 2022).

Multiple enzymes are involved in the synthesis of polysaccharides and affect their content and structural characteristics through mutual balance. Yu et al. discovered that the expression levels of UDP glucose 4-epimerase (UGE) correlated well with the polysaccharide content of Dendrobium officinale at various developmental stages. Glucose and galactose contents increased as a result of high expression of the UGE gene under osmotic and salt stress. Furthermore, improved tolerance was accompanied by less decrease in root length and fresh weight growth, while the content of malondialdehyde (MDA) and proline, which are stress indicators, increased slowly (X. Zhang et al., 2019).

Lycii fructus (Goji berry or Wolfberry), the berry-type fruit of the solanaceous shrubbery *Lycium barbarum* L., has long been highly regarded in international cuisine for its significant contributions to functional dietary tonic. This is due to its widely recognized therapeutic and healthcare benefits including immunoregulation, anti-aging properties, hepatoprotection, eyesight protection, and cancer prevention (Liang et al., 2024). With the gradual popularization of the concept of "preventive treatment for diseases" and an increasing pursuit of healthy longevity, there has been a remarkable surge in the consumption of L. fructus due to its nutritive and preventive therapeutic properties for various health issues.

L. fructus is rich in various metabolites, including polysaccharides, carotenoids, flavonoids, betaine, polyphenols, and other compounds. Among these compounds, the predominant ingredient, solvable L. fructus polysaccharides (LFPs), which have been extensively studied through interdisciplinary research and found to possess multifaceted bioactivities such as antitumor effects, antioxidative properties, anti-aging effects, immunomodulatory functions, and gut microbial modulation capabilities (Zhang, Zhang, et al., 2022).

LFPs are complex polysaccharides exhibiting significant diversity in the structural characteristics. Typically, the representative structure backbone of LFPs consists of a linear homogalacturonan (HG) backbone flanked by alternating sequences of Rhamnogalacturonan- I(RG-I) linkers. The twisted "hairy regions" along the backbone axis are organized by neutral sidechains such as arabinogalactan, arabinan or galactan, which are connected with unique linking glycosidic bonds including α (1–4), β (1–3), β (1–4), β (1–6), et al. (Wang et al., 2024).

The L. fructus cultivated in the Ningxia Hui Autonomous Region was traditionally considered as "authentic", representing high-quality materials from specific geographic regions with unique external ecosystems. In recent years, in order to meet the growing demand for L. fructus and alleviate supply shortages, extensive introduction and cultivation of L. *barbarum* L. have been carried out in various regions of northwest China, including Xinjiang Uygur Autonomous Region, Qinghai province, Inner Mongolia autonomous region, and Gansu province. However, one of the greatest concerns regarding the allopatric cultivation is whether L. fructus was able to withstand the varied external natural conditions and provide stable pharmaceutical values withstand. Indeed, due to factors such as long-term evolution, geographical isolation, genetic drift, etc., L. *barbarum* L. with the same genotype has undergone significant differentiation to adapt to different ecological environments. Consequently, variations in plant and fruit morphology, yield types, and accumulation of endogenous active components exist among different regions due to these environmental differences. These environment-associated differences have prompted researchers to investigate the relationship between the formation and accumulation of various metabolites in L. fructus and external environmental factors.

In order to provide scientific evidence for this traditional belief and recognition based on practices, our research group collected L. fructus samples from various regions and discovered distinct variations in total carotenoid, β-carotene, total phenolic, total flavonoid, total polysaccharide, rutin and ferulic acid contents depending on their geographical origins (Lu et al., 2019). Furthermore, employing an electronic tongue equipped with seven sensors for sensory evaluation enabled us to differentiate samples from different cultivation regions based on taste profiles (sourness, saltiness, freshness, sweetness, and bitterness), indicating further diversity in metabolite composition profiles among these samples (D. Chen et al., 2020). Recently, our group found that polysaccharide-rich water-extracts of L. fructus from NX exhibited superior therapeutic effects against $NaIO_3$-induced visual damaged mice compared to samples from other regions through multivariate statistical analysis of 17 pharmacodynamic indices including retinal apoptosis, oxidative stress levels, the expression of inflammatory mediators, and angiogenic markers (Chen, Guo, et al., 2024).

It is worth noting that while traditional beliefs may associate specific qualities or characteristics with authentic NX-growing L. fructus, there have been limited investigations into the impact of ecological environments on the biosynthesis and structural features of LFPs. Many important questions remained unanswered regarding their structure disparities and underlying regulation mechanisms across different cultivation regions. Consequently, it is imperative to understand the internal and external mechanisms of action by which the biosynthesis and accumulation of LFPs were affected. Based on previous findings, we postulated that the geographical characteristics of cultivation regions may exert an influence on the expression of genes and proteins involved in polysaccharide synthesis, leading to variations in both polysaccharide content and monosaccharide composition. Therefore, our primary objective was to investigate the impact of ecological contexts on upstream LFP genes and downstream LFP product biosynthesis. To fulfill, GC–MS analysis was used to reveal and compare the detailed disparities in monosaccharide constituents within polysaccharides from various regions. Additionally, transcriptomic and proteomic analyses were employed to discover and dissect pivotal candidate genes and proteins implicated in polysaccharide production and compare their synthesis discrepancies. Finally, correlation analysis enabled us to ascertain genes and proteins associated with both polysaccharides and monosaccharides. This research will help in understanding the important material basis and environmental response mechanism for the quality formation of L. fructus, and providing scientific support for the rational development and layout of L. fructus resources.

2. Materials and methods

2.1. Materials

L. fructus samples were of the same genotype "Ningqi No.1" with the same growing ages of 8 years to shield any uncertainties of external disturbances from genetic diversity and/or planting durations. In detail, L. fructus were collected in succession from July 2022 to August 22 in Yinchuan Plain in NX Hui Autonomous Region (abbreviated as NX, N38°40′, E106°03′, 1126 m asl), Delight City in QH Province (abbreviated as QH, N37°23′, E97°22′, 2996 m asl), Jingle County in XJ Uygur Autonomous Region (abbreviated as XJ, N44°36′, E82°54′, 320 m asl). For collection, fruits free from any disease or mechanical injury in the

sunward side were cleaned with sprayed distilled water, dried with neutral filter paper, rapidly frozen in dry ice and then transported in cold chain logistics system to −80 °C freezer in Nanjing University of Traditional Chinese Medicine. Identification was accomplished by Dr. Jintao Duan based on the morphological characteristics and histological standards of Chinese Pharmacopoeia (2020 version).

All the chemicals and reagents were of the highest grade available unless otherwise specified.

2.2. LFPs extraction and content quantification

The total water-soluble LFPs were extracted from L. fructus following a previously protocol with subtle modifications (F. Zhang et al., 2020). 12 fruits randomly picked from 12 independent plants in each collection region were used as biological replicates, forming a total of 36 tested fruits as shown in the simplified diagram of sample collection and replicates selection in Supplementary Fig. S1. Briefly, fruits were first independently smashed and refluxed twice with acetone-petroleum ether at 55 °C for 1 h, followed by refluxing with 80 % ethanol twice at 75 °C for 2 h to remove pigments and small molecules. The LFPs were then extracted by two times water extraction with 20 folds (*w/v*) distilled water at 90 °C for 2 h each time. After freeze centrifuge at 12, 000 ×*g* for 20 min at 4 °C, the supernatant was condensed in a refrigerated vacuum concentrator, washed thoroughly with 75 % ethanol and freeze-dried. By utilizing glucose solution as a standard, the contents of LFPs were measured at 490 nm using the phenol sulfuric acid method.

2.3. Monosaccharide and uronic acid composition assays

For the analysis of monosaccharide and uronic acid composition, the LFPs were dissolved and hydrolyzed in 2 M TFA at a temperature of 110 °C for a duration of 2 h. Subsequently, the liberated monosaccharides were converted into corresponding alditol acetates, while the uronic acids were transformed into N-propylaldonamide acetate derivatives (Wang et al., 2017).

To analyze the derivatives, 2 μL of the prepared samples were separated on an Agilent HP5 ms capillary column (30 m × 0.25 mm × 0.25 μm) installed on an Agilent 7000C GC/MS Triple Quard system (Agilent Technologies, Santa Clara, CA, USA) with a previously reported program (F. Zhang et al., 2020). The data were processed using MassHunter workstation version B.03.01. The quantification was performed by referencing the known concentrations of mix standards (National Institute for Food and Drug Control, Beijing, China).

2.4. Transcriptomic analysis

2.4.1. RNA extraction, RNAseq library preparation and sequencing

For transcriptomic analysis qRT-PCR validation, 3 independent biological replicates from each cultivation region were randomly selected. Total RNA was extracted from L. fructus freeze-dried fruits with TRIzol Reagent (Invitrogen Co., Carlsbad, USA). The concentration and purity of the extracted RNA were determined using ND-2000 (NanoDrop Technologies, Wilmington, USA). The integrity of RNA was assessed by agarose gel electrophoresis, and the RNA Integrity Number (RIN) value was determined with an Agilent 2100 system (Agilent Technologies, Santa Clara, USA). 1 μg of total RNA was used to create a transcriptome library in accordance with TruSeqTM RNA sample preparation kit (Illumina, San Diego, USA). First, the mRNA was enriched with Oligo (dT) magnetic beads and then randomly fragmented into small fragments of approximate 300 bp in size. Next, under the action of reverse transcriptase, it was transcribed into cDNA. After that, the end of the cDNA was repaired, A-tailed, and sequenced, purified, and amplified by PCR to create a cDNA library. Finally, the sequencing was conducted using the Illumina NovaSeq6000 sequencer (Illumina, San Diego, USA) (R. Zhang et al., 2024).

2.4.2. RNA-seq data analysis, annotation and differential expression

The paired-end reads were trimmed and quality controlled using fastp (https://github.com/OpenGene/fastp) with default parameters. The clean data from the samples were used for de-novo assembly with Trinity (http://trinityrnaseq.sourceforge.net/), and the Fragments Per Kilobase of transcript per Million mapped reads (FPKM) value was calculated to quantify the expression. All transcripts were annotated using databases, including the Gene Ontology (GO) database, Kyoto Encyclopedia of Genes and Genomes (KEGG) database, NCBI non-redundant (Nr) database, Swiss-Prot protein database, and Pfam database. DESeq2 was used to analyze differentially expressed genes (DEGs). A p value<0.05 and fold change (FC) > 1.5 or FC < 0.65 were set as the thresholds for significant differential expression (Barratt et al., 2023).

2.4.3. qRT-PCR analyses of gene expression levels

The genes involved in LFP biosynthesis were identified using the KEGG pathway annotation dataset, and suitable primers were designed using Premier 5.0 (refer to Table S1 for sequences). After extracting total RNA from L. fructus, the first strands of cDNA were reverse-transcribed using a Prime Script RT Master Mix (Takara, Dalian, China). The synthesized first-strand cDNA was used as a template for qRT-PCR, which was conducted using a CFX96 Real-time PCR Detection System (Bio-Rad, Hercules, USA). Relative expression was analyzed using the comparative $2^{-\Delta\Delta CT}$ method with β-actin as the internal control gene (Gigli-Bisceglia et al., 2022). The experiment involved three biological replicates and analyzed relative expression using the mean and standard deviation (SD).

2.5. Data-independent acquisition (DIA)-based proteomic analysis

2.5.1. Protein extraction and peptide digestion

3 randomly selected biological replicates from each of NX, XJ, and QH, respectively, were subjected to DIA quantitative proteomics. Total protein was extracted using the cold acetone method (Li et al., 2021). In brief, L. fructus fruits were crushed in liquid nitrogen, and added with protein lysis solution (100 mM ammonium bicarbonate, 6 M urea, 0.2 % SDS, pH = 8), and shook it to ensure complete decomposition. After centrifuging at 12,000 ×*g* at 4 °C for 15 min, the supernatant was reduced and alkylated with 10 mM dithiothreitol (50 °C, 1 h) and iodoacetamide solution (IAM) in the dark for 1 h. Added pre-cooled acetone and precipitated the protein at −20 °C for 2 h. After the proteins were precipitated and cleaned the with pre-cooled acetone, protein solubilizer (6 M urea, 100 mM tetraethyl-ammonium bromide, pH = 8.5) was added to dissolve the proteins. Next, protein solutions (100 μL) prepared was digested overnight at 37 °C with lysis buffer containing 3 μL of 1 μg/μL trypsin and 500 μL of 50 mM tetraethyl-ammonium bromide buffer. The digested peptides were acidified with 2 μL of 100 % formic acid to pH < 3 and desalted with a C18-pipette tip.

2.5.2. Peptide separation on reversed phase liquid chromatography

Peptides in 2 % formic acid were loaded onto an Rigol L3000 HPLC system (Thermo Fisher Scientific, Waltham, USA) equipped with a BEH C18 column (5 μm, 4.6 × 250 mm, Waters, Manchester, UK). Peptides were separated on a 0 %–45 % acetonitrile gradient (90 min) with 0.1 % formic acid at a flow rate of 350 mL/min. The peptide ions in the spray were detected and analyzed on a nanospray LTQ Orbitrap Velos mass spectrometer (Thermo Fisher Scientific, Bremen, Germany), which was operated in the positive mode to measure full scan MS spectra (from m/z 350–1800 in the Orbitrap analyzer at resolution $R = 60{,}000$) followed by isolation and fragmentation of the 15 most intense ions (in the LTQ part) by collision-induced dissociation. Eluates were collected every 1 min and a combination of 10 fractions were then frozen and dried.

2.5.3. Data-dependent acquisition (DDA) spectrum library construction and DIA labeling

For the DDA library construction, peptide fractions were loaded on a

C18 Nano-Trap column (2 cm × 75 μm, 3 μm) (Thermo Fisher Scientific, Waltham, USA) after mixed with standard peptides (Biognosys, Schlieren, Switzerland). DDA-MS analysis was conducted by utilizing full scans of Q Exactive™ HF-X (Thermo Fisher Scientific, Waltham, USA) with a Nanospray Flex™ (ESI) ion source. The topmost 40 intense precursor ions were fragmented by higher energy collisional dissociation for DDA spectral library.

LC-MS/MS analysis in DIA mode was performed on a packed analytical column (75 μm × 50 cm) affiliated to the EASY-nLC™ 1200 UHPLC system coupled with an Orbitrap Q Exactive HF-X mass spectrometer (Thermo Fisher Scientific, Waltham, USA) with a gradient elution program. The peptides were separated using two mobile phases: solvent A (0.1 % (*v*/v) formic acid in water) and solvent B (acetonitrile with 0.1 % formic acid), with a 135 min gradient. Total fractions (1 μg) coupled with 0.4 μL standard peptides were analyzed using the C18 Nano-Trap column (2 cm × 75 μm, 3 μm, Thermo Fisher Scientific, Waltham, USA) in DIA mode.

All labeled samples were mixed with an equal volume of reagent, desalted, and lyophilized. The lyophilized powder was dissolved in mobile phase A (98 % acetonitrile, 2 % water, pH 10.0). The peptides were fractionated using an L3000 HPLC system with a C18 column (4.6 mm × 250 mm, 5 μm, Thermo Fisher Scientific, Waltham, USA). A 1 μg sample was taken from the supernatant of each fraction and separated using an EASY-nLC™ 1200 UHPLC system. The separated peptides were analyzed using a Q Exactive™ HF-X mass spectrometer (Thermo Fisher Scientific, Waltham, USA).

2.5.4. Proteomic data analysis

The resulted spectra from each fraction were searched separately against the L. fructus database using the Proteome Discoverer 2.2 search engine (Thermo Fisher Scientific, Waltham, USA). Spectronaut software was used to achieve simultaneous qualitative and quantitative analysis of proteins. FC $>$ 1.2 and p-value $<$0.05 were used as thresholds to define differentially expressed proteins (DEPs) and further analyze them through Gene Ontology (GO) and Kyoto Encyclopedia of Genes and Genomes (KEGG) enrichment analysis.

2.6. Data analysis, statistics, and mapping

The longitude and latitude coordinates of each sampling point were collected in the "Traditional Chinese Medicine Resource Spatial Information Network Database," along with 51 ecological factors such as soil type, temperature, precipitation, radiation, etc. (43 climate factors and 8 soil factors). The data was expressed as mean ± standard error (SD), representing the average and SD of a minimum of three biological replicates conducted under similar conditions. Statistical analysis was performed using one-way analysis of variance (ANOVA) followed by Dunnett's multiple comparison tests. A significance level of $P < 0.05$ was set to determine statistically significant differences. To elucidate the relationship between variables, Simca 14.1 software was utilized for conducting principal component analysis (PCA) and a supervised partial least-squares discriminant analysis (PLS-DA) clustering method to transform the original variables into linear combinations. Variables with a Variable Importance in Projection (VIP) greater than 1.0 were considered responsible for the separation observed in the analyses. Bivariate correlation analysis was carried out using SPSS 19 data matrix software. Differential heat maps were generated using TBtools.

3. Results and discussion

3.1. Determination of LFP content in different cultivation regions

The L. fructus samples were collected from three distinct cultivation regions, namely NX, XJ, and QH, to represent both the traditional "authentic" and emerging cultivation regions. It is worth noting that all the samples belonged to the same genotype called "Ningqi No.1," which has shown remarkable efficacy in modulating $NaIO_3$-induced retinal degeneration in mice (Chen, Wei, et al., 2024). Furthermore, the fruits were obtained from plants of identical growth and fruiting years to eliminate any potential interfering factors.

The contents of different LFPs were determined and compared using the classical phenol sulfuric acid method. Although comparable concentrations of LFPs were found in XJ and QH (33.10 mg and 33.70 mg per gram fresh fruit weight or 3.31 % and 3.37 % as expressed in Fig. 1A, respectively), a significant difference was observed between the samples from NX and those from the other two regions ($p < 0.05$). Specifically, the LFP content in NX was significantly lower at 0.94 % compared to XJ and QH.

3.2. Analysis of monosaccharide composition and proportion in LFP

The monosaccharide and uronic acid composition played a crucial role in characterizing the structure of LFPs. Therefore, qualitative and quantitative analysis of the monomer composition profile was simultaneously achieved using GC–MS spectrometry after TFA hydrolysis and pre-column glycol-acetate derivation. As depicted in Fig. 1B through GC–MS profiles and summarized as molar ratios (%) in Table 1 and Fig. 1C, there were no significant differences observed among the types of composed monosaccharides and uronic acids across the 36 samples. The predominant monomeric compositions consisted mainly of Glc, Ara, Gal, and GalA with moderate amounts of Rha, Man, Xyl, and GlcA. This indicated that LFPs exhibited heterogeneity in their chemical structures. Notably, an abundance of Glc served as a strong indicator for the presence of cellulose or hemicellulose. Conversely, high ratios of Ara, Gal, and GalA suggested an enrichment of neutral (Ara + Gal) monosaccharides within branched RG-I moieties flanked by fairly long linear HG backbones, the characteristic components found in acidic heteropolysaccharides such as pectin matrices. This coexistence supported the new paradigm where cells do not exist as isolated islands surrounded by insulative cell walls; instead, the cytoplasmic region along with plasma membrane and cell wall form a continuum, wherein each constituent actively participates in various cellular processes including growth, development, and recognition (Leszczuk et al., 2018).

To clarify the structural similarity and diversity of LFPs, the approximate percentages of HG were estimated using the following formulas: HG% = GalA (%) – Rha (%).

Despite the similarity in constituent monosaccharide types, the influence of the growing environment on the chemical structures of LFPs was evidenced by the detailed molar ratio of their composing monomers. LFPs from NX exhibited significantly higher levels of HG moieties compared to those from XJ and QH. Upon careful examination, it was apparent that this enrichment in structural feature primarily arisen from elongated linear HG aggregation rather than variations in Rha percentage. This phenomenon can be attributed to the inherent sensitivity of HG towards environmental changes and its susceptibility to environmental modifications for achieving structural and functional adaptations (Rial-Hermida et al., 2021). Additionally, considering that neutral monosaccharides Ara and Gal typically form arabinans, galactans, and arabinogalactans as predominant side chains within RG-I domain, the significant decrease in Ara + Gal content observed in XJ samples further elucidated the susceptibility of LFPs towards environmental influences.

To compare the content and chemical structure composition of LFPs from different cultivation regions, datasets obtained from content analysis and GC–MS were subjected to successive PCA and PLS-DA as shown in Fig. 1D and E, respectively. In the PCA score plot, two components accounted for 58.8 % and 17.7 % of the total variance, respectively. The samples from the same region clustered tightly together while clear discrimination was observed among samples from NX and the two other regions, indicating significant differences in LFPs between NX, XJ, and QH. Four factors, namely LFPs content as well as molar ratios of Glc, Ara, and GalA, exhibited higher values in VIP

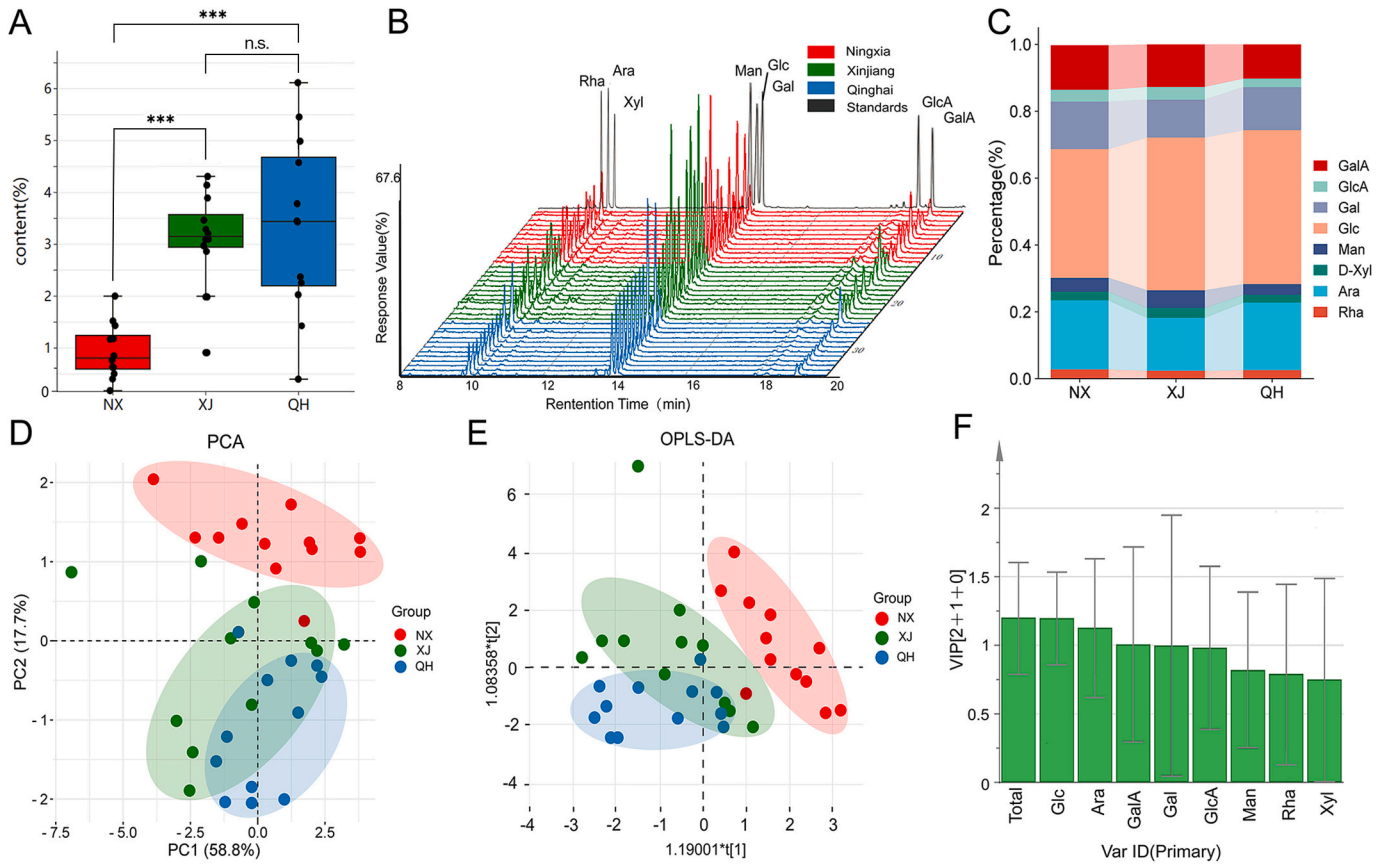

Fig. 1. Overview of polysaccharide content and structures of LFPs from NX, XJ and QH. (A) Column chart of total polysaccharide contents in NX, XJ, and QH (***: $p < 0.001$, n.s.: no significance); (B) GC–MS total ion flow in NX, QH, and XJ; (C) Stacking diagram of the content of various monosaccharide components in polysaccharides from NX, XJ, and QH; (D) PCA chart of monosaccharide content in three production regions; (E) PCA chart of monosaccharide content in three production regions; (F) Column chart of VIP values of content and monosaccharide and uronic acid composition of LFPs with a cutoff set at 1.0.

Table 1
The content (% in fresh fruit weight), monosaccharide and uronic acid composition (% in molar ratio) of LFPs.

Collection location	NX	XJ	QH
LFPs content (%)	0.94 ± 0.52	3.30 ± 0.93	3.37 ± 1.70
Rha	2.58 ± 0.89	2.38 ± 0.57	2.57 ± 0.42
Ara	19.54 ± 4.12	15.83 ± 2.50	20.21 ± 3.44
Xyl	2.74 ± 1.04	2.97 ± 1.19	2.30 ± 1.32
Man	4.17 ± 1.50	5.31 ± 2.11	3.23 ± 0.82
Glc	37.39 ± 8.93	45.67 ± 7.96	46.05 ± 7.97
Gal	13.48 ± 2.60	11.36 ± 2.53	12.87 ± 3.04
GlcA	3.92 ± 2.90	3.79 ± 1.57	2.52 ± 1.97
GalA	15.97 ± 11.31	12.70 ± 4.76	10.24 ± 4.50
Ara + Gal	33.01 ± 5.89	27.19 ± 3.84	33.09 ± 4.28
HG	18.55 ± 11.02	10.33 ± 4.59	7.67 ± 4.19

screening and could serve as diagnostic distinguishing factors accounting for differences in LFPs originating from different geographical locations (Fig. 1F).

The significant disparities in the content and structural composition reflect the pivotal involvement of LFPs in adapting to various ecological environmental stresses. Specifically, the variation in contents signifies the allocations and distributions between LFPs and other cell wall polysaccharides, primarily cellulose and hemicellulose. Moreover, the diagnostic distinguishing factors Glc, Ara, and GalA are derived from HG and neutral side chains of polysaccharides, respectively. This implies that these structural moieties organize in different proportions as response and adaptation strategies when integrated into complex polysaccharide structures.

3.3. Transcriptomic analysis of L. fructus from three various cultivation regions

Nine RNA-seq libraries were prepared and sequenced from three cultivation regions of L. fructus, resulting in a total of 57.68 Gb of clean data after filtration. For each sequencing sample, the clean reads and smallest length were 6.09 Gb and 201 bp, respectively, with Q30 bases accounting for more than 93.48 %. A total of 82,225 genes were detected across the 9 samples, with an average N50 length of 1571 bp and a GC content of 39.64 %. Based on the RNA level chart, the gene expression levels of L. fructus in NX, XJ, and QH exhibited relative consistency. PCA analysis revealed clear clustering of the three duplicate samples from NX and XJ (Fig. 2A). Although the three repeated samples in QH showed slight scattering, the correlation between gene expression levels among all samples indicated a Pearson correlation coefficient squared (R2) greater than 0.8, confirming that the transcriptome data met subsequent analysis requirements (Fig. 2B). The Venn diagram visually depicted gene differences in L. fructus among the three different cultivation regions; specifically expressed genes were most abundant in XJ while least abundant in QH (Fig. 2C). In XJ, a total of 5531 differentially expressed genes (DEGs) were identified; out of these DEGs, 3043 exhibited substantial upregulation while 2488 showed significant downregulation. In comparison to NX, QH had a total of 8084 DEGs; among them, there were 3957 significant upregulated and 4127 significant downregulated genes (Fig. 2D).

3.4. Proteomic analysis of L. fructus from three various cultivation regions

In order to further validate the findings at the protein level, we

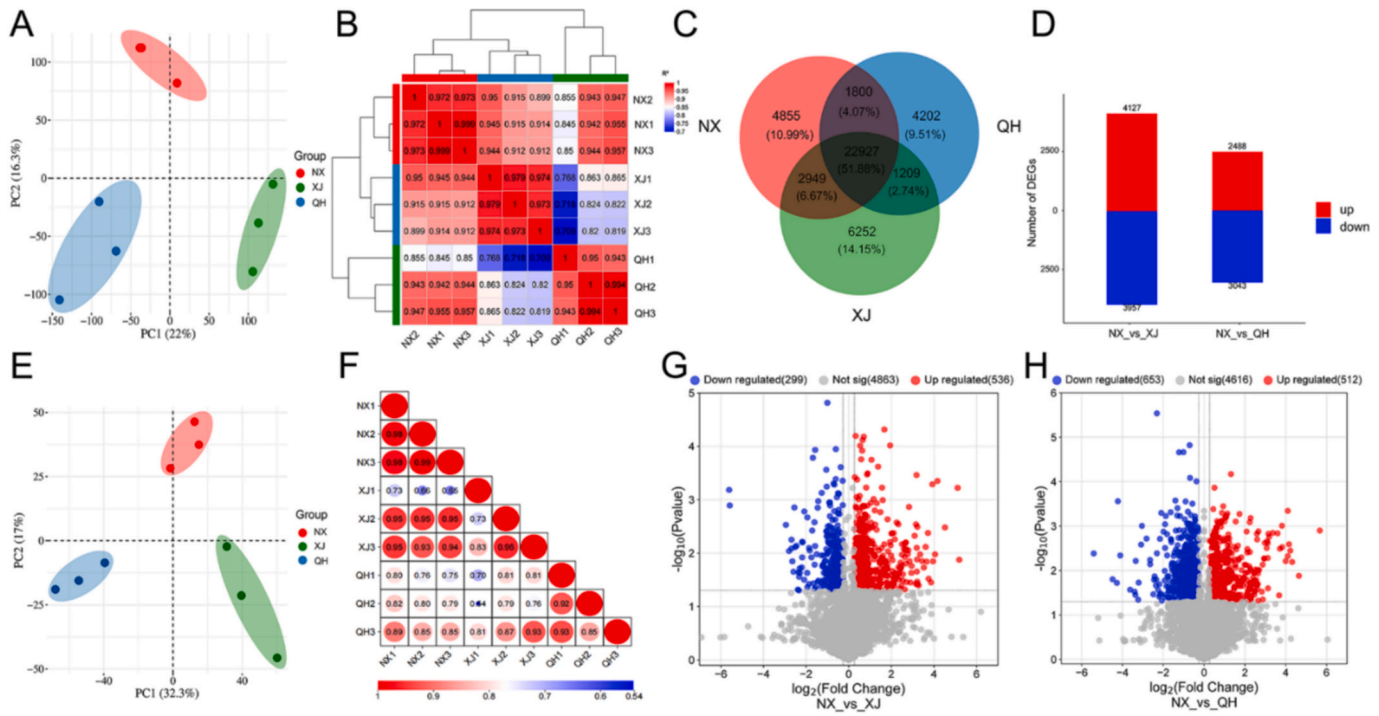

Fig. 2. Overview of transcriptomic and proteomic data; (A) Transcriptome PCA score chart; (B) Correlation heatmap between three repeated transcriptomic samples in NX, XJ, and QH; (C) Venn map of genetic differences in NX, XJ, and QH; (D) Differentially expressed genes with NX as the control group; (E) Proteome PCA score chart; (F) Correlation heatmap of three repeated proteomic samples in NX, XJ, and QH; (G) Volcanic plots of DEPs between NX and XJ; (H) Volcanic plots of DEPs between NX and QH.

conducted DIA quantitative proteomics analysis on L. fructus samples collected from NX, XJ, and QH regions. A total of 340,695 spectra were generated in this study. After excluding peptide segments and proteins with a false discovery rate (FDR) exceeding 1 %, a total of 7798 proteins corresponding to 40,629 peptides were obtained for further analysis.

PCA of proteomics demonstrated relatively close distances between replicate samples while significant distances were observed between different L. fructus cultivation regions (Fig. 2E). Correlation analysis was carried out among L. fructus samples from different cultivation regions, revealing stronger correlation and better reproducibility within the same cultivation region. However, poor correlation was observed between various cultivation regions indicating significant differences in L. fructus from NX, XJ, and QH (Fig. 2F). Based on defined difference threshold values, a total of 3728 differentially expressed proteins (DEPs) were identified in the XJ region and 4732 DEPs in the QH region through comparative analysis (Fig. 2G and H).

3.5. COG and KEGG analysis of differentially expressed genes and proteins

The DEPs in each group were analyzed using the COG and KEGG databases to gain insights into the key biological processes in L. fructus. According to the COG annotation analysis, the top 5 DEGs included posttranslational modification, protein turnover, chaperones; transcription; signal transduction mechanisms; replication, recombination and repair; and carbohydrate transport and metabolism (Fig. 3A). Notably, significant differences in genes related to carbohydrate transport and metabolism were observed among different cultivation regions. Furthermore, KEGG enrichment analysis revealed that the top 5 pathways involved in 'carbohydrate transport and metabolism' were amino sugar and nucleotide sugar metabolism, starch and sucrose metabolism, pyruvate metabolism, pentose and glucuronate interconversions, glycolysis/gluconeogenesis as well as glyoxylate and dicarboxylate metabolism (Fig. 3B & Fig. 3C). Interestingly enough, these metabolic pathways align with previously reported polysaccharide synthesis pathways which indicate substantial genetic variations in polysaccharide synthesis between NX region compared to other cultivation regions. Additionally noteworthy is that both comparison groups exhibited enrichment of the MAPK signaling pathway along with plant-pathogen interaction - two crucial components involved in enhancing stress resistance through plant defense mechanisms.

After analyzing the top 5 COG annotations on DEPs, significant differences were primarily observed in pathways related to translation, generic structure and biogenesis; general function prediction only; posttranslational modification, project turnovers, chambers; carbohydrate transport and metabolism; as well as lipid transport and metabolism (Fig. 3A). Evidently, substantial disparities existed in protein-mediated carbohydrate transport and metabolism across different cultivation regions. Furthermore, KEGG enrichment analysis of the top 5 pathways revealed notable enrichment in polysaccharide synthesis pathways such as starch and sucrose metabolism, glycolysis/gluconeogenesis, and amino sugar and nucleotide sugar metabolism (Fig. 3D and E). The findings from transcriptome and proteome analyses support variations in gene expression levels and protein abundance during polysaccharide synthesis among XJ, QH, and NX. These discrepancies may consequently impact downstream polysaccharide content as well as monosaccharide composition variations.

3.6. The synthesis pathway of sugar nucleotides in polysaccharides

To enhance our understanding of L. fructus polysaccharide biosynthesis, the relevant genes and protein in LFPs biosynthesis pathway were investigated through annotation with the KEGG database.

In the initial two steps of polysaccharide synthesis, a total of 70 genes and 39 proteins were identified(the identified genes and proteins were shown in Supplementary Fig. S2 and the significant DEGs and DEPs were shown in Fig. 4A and B, respectively), including sucrose-phosphate synthetase (SPS), subcrosse-6-phosphate synthetase (SPP), sucrose

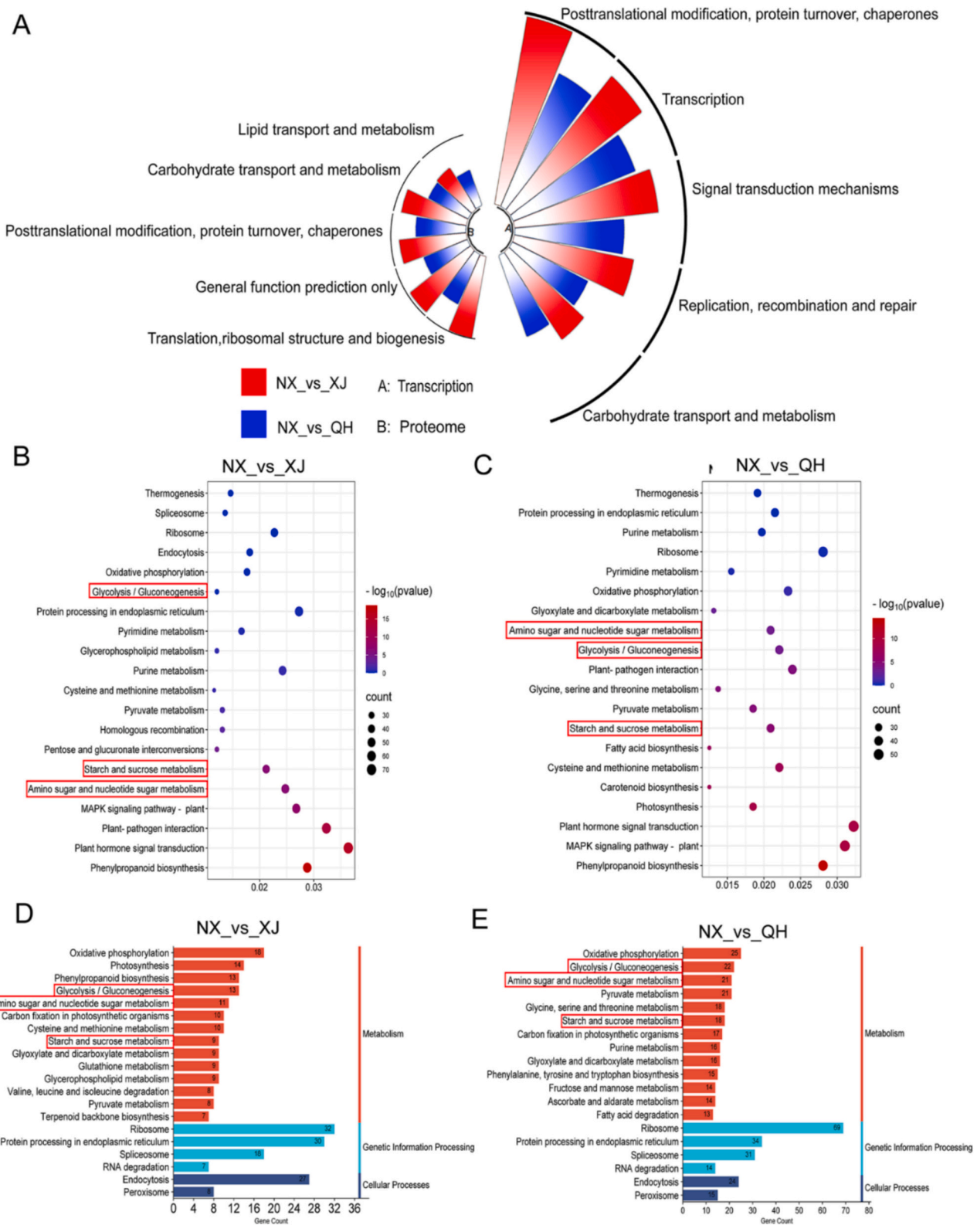

Fig. 3. COG and KEGG analysis of differentially expressed genes and proteins. (A) The top five differential pathways obtained from transcriptome and proteome COG differential analysis; (B) Top 20 path bubble charts generated from KEGG analysis of differences between NX and XJ in the transcriptome; (C) Top 20 path bubble charts obtained from KEGG analysis of the differences between NX and QH in the transcriptome;(D) The top 20 pathway bar charts obtained from KEGG analysis of differences in the proteome between NX and XJ; (E) The top 20 pathway bar charts obtained from KEGG analysis of differences in the proteome between NX and QH.

synthetase (SUS), beta-fructofuranosidase (INV), hexokinase (HK), fructokinase (scrK), phosphoglucomutase (PGM), UTP-glucose-1-phosphate uridylyltransferase (UGP2), fructokinase (FRK), glucose-6-phosphate isomerase (GPI), mannose-6-phosphate isomerase (MPI), phosphomannomutase(PMM), mannose-1-phosphate guanylyltransferase(GMPP), GDP-mannose 4,6-dehydratse(GMD), UDP-glucose 6-dehydrogenas(UGDH), galactose dehydrogenase(UGD), UDP D -xylose synthase(UXS), UDP-arabinos4-e epimerase(UXE), UDP-apiose/xylos synthase(AXS), UDP-glucose A-4-epimerase(GAE) and UDP-glucos 4,6-dehydratas(RHM). The synthesis of LFP may be co-regulated by multiple genes and proteins, with L. fructus from different regions exhibiting varying levels of gene expression and protein abundance in different cultivation regions. Notably, the expression levels of INV, SUS, UGP2, and PGM in both coding genes and proteins were relatively high which could potentially account for the elevated glucose percentage.

UTP-glucose-1-phosphate uridylyltransferase (UGP2, EC 2.7.7.9) catalyzes the conversion of glucose 1-phosphate and UTP into UDP-glucose, which serves as a donor of glucose residues (Yuan et al., 2022). This enzyme plays a pivotal role in carbohydrate metabolism and cell wall biosynthesis. In the transcriptome analysis of QH, three genes were identified, with only one gene exhibiting consistent expression patterns in both the transcriptome and proteome datasets. The remaining two genes showed upregulation at the transcript level but downregulation at the protein level. Additionally, mutase (PGM), another crucial enzyme involved in nucleotide sugar precursor biosynthesis pathway, can significantly impact polysaccharide biosynthesis when overexpressed. In QH's transcriptome data, three PGM genes were identified; two of them displayed concordant expression patterns

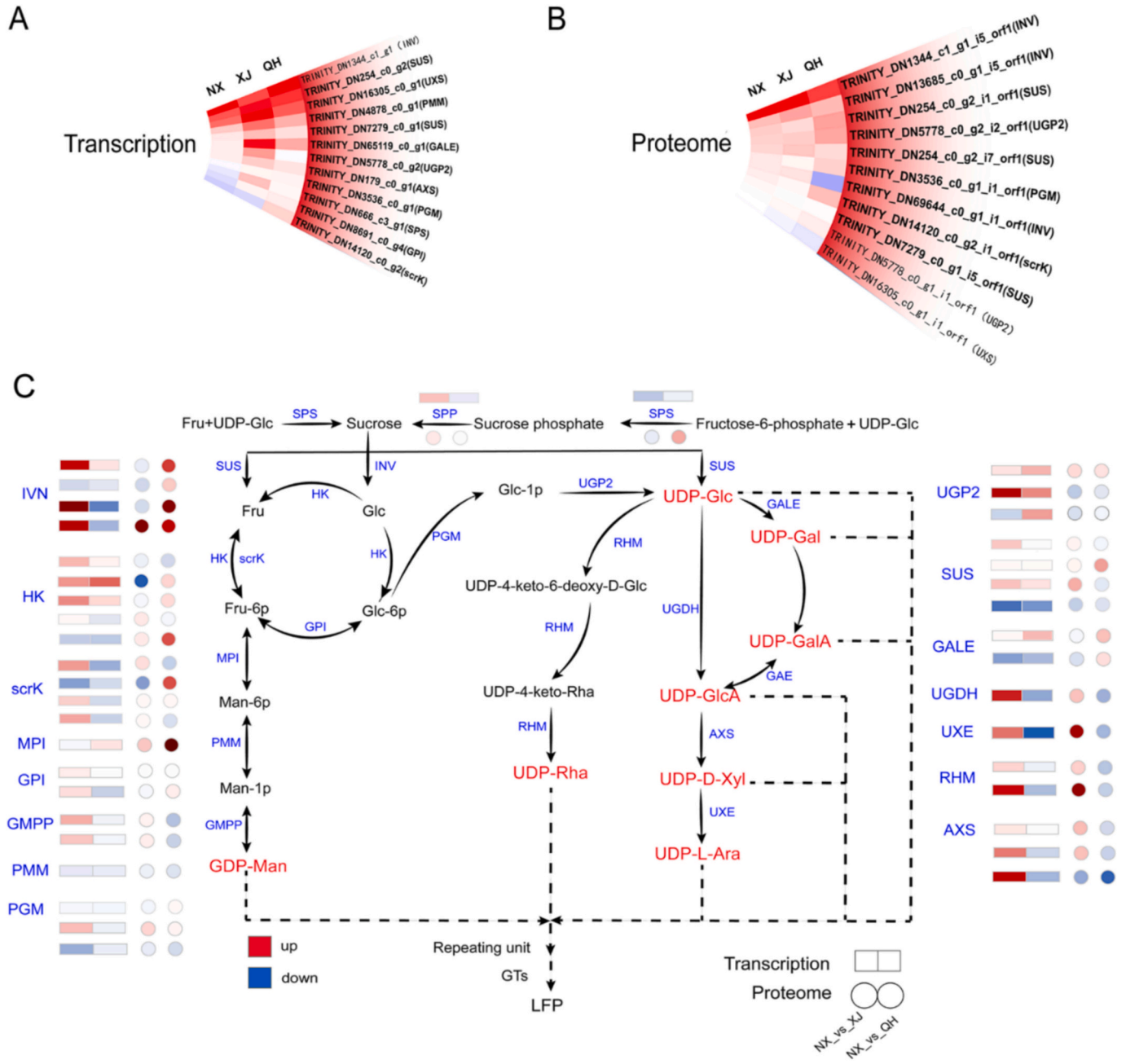

Fig. 4. Identified genes, proteins and proposed pathways for LFPs synthesis. (A) Selective cluster heatmap of polysaccharide synthesis-related genes in transcriptome. (B) Selective cluster heatmap of polysaccharide synthesis-related proteins in the proteome. (C)Proposed pathways for LFPs biosynthesis in L. fructus form different cultivation regions.

between the transcriptome and proteome datasets while one gene exhibited discordant expression patterns between these two datasets (Fig. 4C). These findings suggest that complex regulatory mechanisms may be involved in gene expression and mRNA undergoes various modifications during translation into proteins, leading to inconsistencies between transcriptomic and proteomic data.

3.7. The synthetic pathway of polysaccharide polymerization

The glycosylation process in polysaccharide polymerization represents the final stage in the biosynthesis of most plant quality markers, with glycosyltransferases (GTs) serving as crucial enzymes (Wang et al., 2019). GTs facilitate the transfer of monosaccharide residues from active nucleotide sugars to elongated polysaccharide chains, enabling dehydration and condensation reactions that lead to polysaccharide formation (Ebert et al., 2019; Takenaka et al., 2019). Transcriptome analysis identified 104 related genes for glucosyltransferases along with 8 for rhamnosyltranferases, 13 for arabinosytranferases, 18 for xylosytranferases, 18 for mannosytranferases, 36 for galactosytranferases, 30 for glucuronyltransfereases, and 32 genes related to galacturonoyltraneserfes. On the other hand, proteome analysis only identified 20 proteins related to glucotransferases, three proteins related to xylostransferases, two proteins related to mannose transferases, one protein related to galactosyltransferases, five proteins related to glocurnoysltanfsresae, and two proteins related to galacturonosyltransferases (Fig. 5A and B).

In L. fructus, 98 GTs related genes and 12 GTs related proteins were annotated, including ARAD1, RAY1, HPAT, XEG113, RRA for Ara synthesis; MGP4 and XGD1 for Xyl synthesis; GlcAT14 for GlcA synthesis; GAUT and GATL for GalA synthesis; RRT1 for Rha synthesis; and GALS, GALT, HPGT, SGT for Gal synthesis. The relatively low number of glycosyltransferases identified through annotation may be attributed to the fact that L. fructus has reached full maturity stage resulting in a significant decrease in sugar biosynthesis as well as weakened degradation metabolism of cell wall polysaccharides and starch. HG moiety in acidic polysaccharides is synthesized by members of the galactosyltransferase family such as GAUT6/8/9/1: GAUT7 complex while RG-I is associated with the activity of enzymes like RRT1, ARAD1/2 and GALS. Side chain AG is linked to the function of enzymes such as RAY1/GALT2/GLCAT14A/GALT31A whereas RG-II biosynthesis only involves MGP4.

Studies have demonstrated that enzymes involved in polysaccharide synthesis play a crucial role in regulating both the production and composition of monosaccharides. To ensure result reliability, we chose to analyze a positive correlation between protein abundance and transcript accumulation since their genes were either unregulated or regulated to a lesser extent at post-transcriptional or translational levels (Fig. 5C and D). Genes and proteins with similar expression patterns during polysaccharide synthesis were analyzed: six genes and proteins including scrK5, SUS6, AXS2, INV1, UXE, RHM1, GAUT8 and GAUT9 in XJ as shown in Fig. 5C, while four genes and proteins including UGDH1, AXS1, RHM1and scrK2 in QH as shown in Fig. 5D.

The assembly of functional plant polysaccharides remains poorly understood in general, primarily due to the challenges associated with studying the diverse constituents and complex processes involved. This intricate process necessitates a series of enzymes that facilitate the conversion of photosynthetically produced sucrose into various polysaccharides through sucrose conversion, UDP monosaccharide transformation into other NDP monosaccharides, and subsequent polymerization of polysaccharides (Verbančič et al., 2018).

The KEGG annotation in the current study identified a total of 59 enzymes in polysaccharide synthesis pathway, comprising 39 for the initial two steps and 20 for polysaccharide polymerization. These enzymes exhibited significant enrichment, providing further evidence for the crucial regulatory roles of UDPs, AXS, and UGDH. Notably, UGDH is implicated in the biosynthesis of UDP-GlcA through an NAD^+-dependent redox chemistry process, thereby inhibiting UDP-GlcA synthesis and reducing GalA content (Ma et al., 2023). This reduction is particularly important as GalA serves as a major sugar residue in pectic polysaccharides. Consistent with the GC–MS-based composition patterns of LFPs, the expression level of UGDH was significantly lower in NX compared to QH, partially explaining the elevated levels of GalA content and HG moieties observed in NX's LFP chemical structures.

Another example is AXS, an essential enzyme that specifically catalyzes the conversion of UDP-GlcA to UDP-D-xylose and subsequently to UDP-L-Ara (Zhang et al., 2021). The expression of AXS may be responsible for the incorporation of Ara into pectin and hemicellulose polysaccharides, as well as the accumulation of individual LFPs under environmental stress. Herein, we observed a higher transcription level of AXS in QH compared to NX, while XJ exhibited a lower transcription level. This finding explains the elevated percentage of Ara in QH LFPs and the decreased percentage in XJ LFPs.

Although various enzymes have been identified through the integration of high throughput omics data, it is worth noting that currently, none of these biosynthetic enzymes have undergone purification and functional verification. Further studies are required to uncover the mechanistic inter-relationship between enzymes and LFPs structure, which remains undisclosed at present. To overcome these challenges, certain emerging strategies may contribute to their identification. For instance, genetic techniques have successfully been employed in identifying several genes involved in pectin biosynthesis, which could be applied to elucidate LFPs biosynthesis as well (Vaahtera et al., 2019). Furthermore, additional investigation is needed to determine the synthesis and accumulation of LFPs and their impact on biological activities in terms of both presence and extent. Characterization of the screened genes may provide a foundational basis for future endeavors aimed at identifying other crucial enzymes involved in polysaccharide

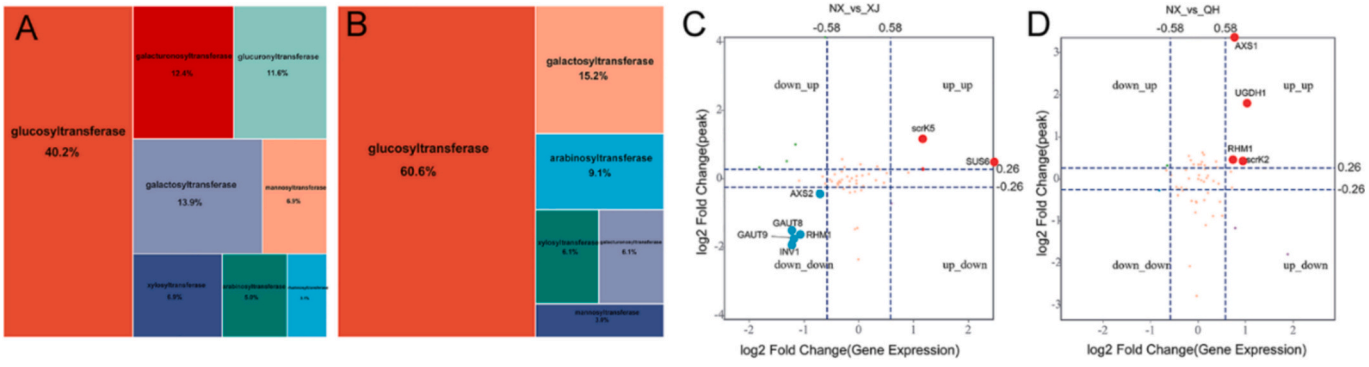

Fig. 5. Number of genes and proteins involved in polysaccharide polymerization in LFPs synthetic pathway of L. fructus from different regions. (A) and (B) The number of glycosyltransferases annotated in the transcriptome and proteome, respectively. (C) and (D) Nine quadrant diagram of polysaccharide genes and proteins in NX vs XJ, NX vs QH, respectively.

biosynthesis under different environmental conditions.

3.8. qRT-PCR analysis

To further validate the comparative results that showed high regulation in LFPs biosynthesis, 11 up- and downregulated unigenes in polysaccharide synthesis pathway were randomly selected for qRT-PCR analysis to determine the expression levels, using the same samples for transcriptomic sequencing. Although slight variations were observed in a few genes compared to their RNA-seq expressions, good correlation was found between RNA-seq and qRT-PCR results ($R^2 = 0.824$; $p < 0.001$, Fig. 6), which further confirmed the reproductivity and reliability of RNA Seq gene expression data and verifies the expression levels of structural genes related to LFPs synthesis. Moreover, there was a significant variation in gene expression between NX, XJ and QH regions, with some genes showing higher expression levels such as INV, SUS, UGP2 and PGM. This differential pattern may account for differences in LFPs synthesis and accumulation between these two cultivation regions, and may play important roles as key genes involved in LFPs biosynthesis and accumulation for further understanding procedure of environmental adaptation and the quality formation of L. fructus.

3.9. The effect of environmental factors imposed on DEGs, DEPs and LFPs structures

Mantel test was employed to characterize the association between relevant genes and environmental factors, extracting groups with correlation coefficients greater than or equal to 0.5 for subsequent analysis (Fig. 7A, B and C). Notably, both gene expression and protein levels encoding UXE were higher in NX, potentially enhancing its ability to respond effectively to various pathogen invasions. In XJ, UXE, RHM1, GAUT8, and GAUT9 exhibited significant susceptibility to environmental factors, primarily influenced by temperature from March to October followed by precipitation, displaying a noteworthy positive correlation. In QH, AXS2 and UGDH were significantly impacted by environmental factors. They were mainly affected by temperature from April to November followed by precipitation with a substantial positive correlation. Interestingly, both the genes and proteins encoding UGDH showed significant upregulation in QH, possibly indicating their role in responding to the unique temperature and precipitation conditions present there. Overall, the genes involved in regulating LFP synthesis were predominantly influenced by temperature and precipitation.

Consistently, a heat map of the environmental factors and LFPs structures demonstrated Ara and GalA percentages showed contrary tendency in associated with temperature and precipitation, while Glc percentage exhibited negative associations with precipitation and temperature (Fig. 7D). Environmental factors not only impacted monosaccharide composition but also significantly influenced polysaccharide content. LFPs contents showed a positive correlation with soil clay content and temperature day-night difference, whereas pH level, soil sand content and temperatures from October to March displayed negative effects.

As was mentioned above, carbohydrate and polysaccharide metabolism are influenced by various abiotic stresses. Plants regulate growth and development by modulating sugar accumulation in response to abiotic stresses. Following the transplantation of L. fructus from NX to XJ and QH, temperature and precipitation exerted an influence on the gene expression and protein levels involved in polysaccharide synthesis process. Consequently, variations occurred in both the total amount of downstream polysaccharides and the composing proportion of monosaccharide components, especially in Glc, Ara, and GalA. Furthermore, although significant differences were observed in the content of these three monosaccharides across different cultivation regions, glucose remained predominant among them. Given its role as a precursor for polysaccharide synthesis along with consistently high molar percentage levels observed here suggests that glucose availability is sufficient for energy production LFPs synthesis.

4. Conclusion

The current research systematically analyzed the structural differences and underlying regulatory mechanisms of soluble polysaccharides in L. fructus from different regions in China through LFPs content determination, monosaccharide composition analysis, and in-depth mining of transcriptome and proteome data. The results unveiled significant variations in both LFPs content and monosaccharide composition among the different production regions, thereinto, the total LFPs content, the percentage of Glc, Ara and GalA explained the main differences among LFPs from the regions. Mechanistically, the structural variations were due to the various expression of enzymes in the synthesis pathways of LFPs, including scrK5, UXE, GAUT8, GAUT9, AXS2, and UGDH. The expression of crucial enzymes involved in the biosynthesis

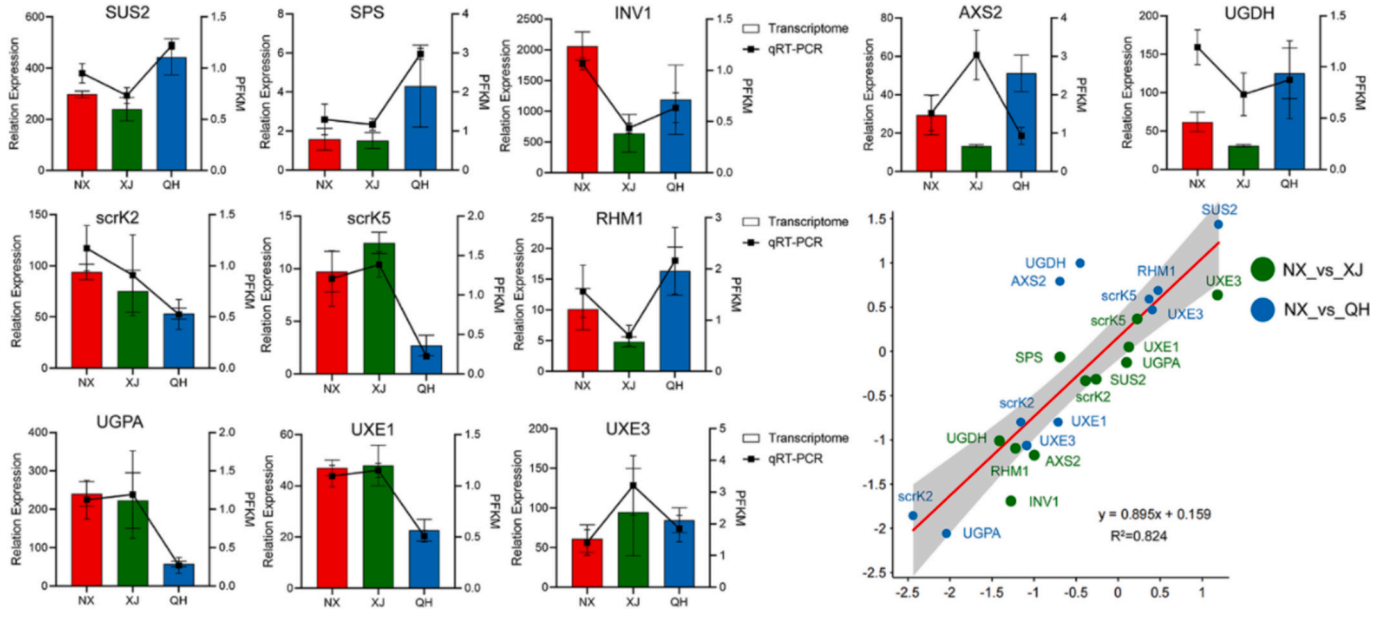

Fig. 6. qRT-PCR validation of 11 LFPs synthesis involved genes of L. fructus from NX, XJ and QH.

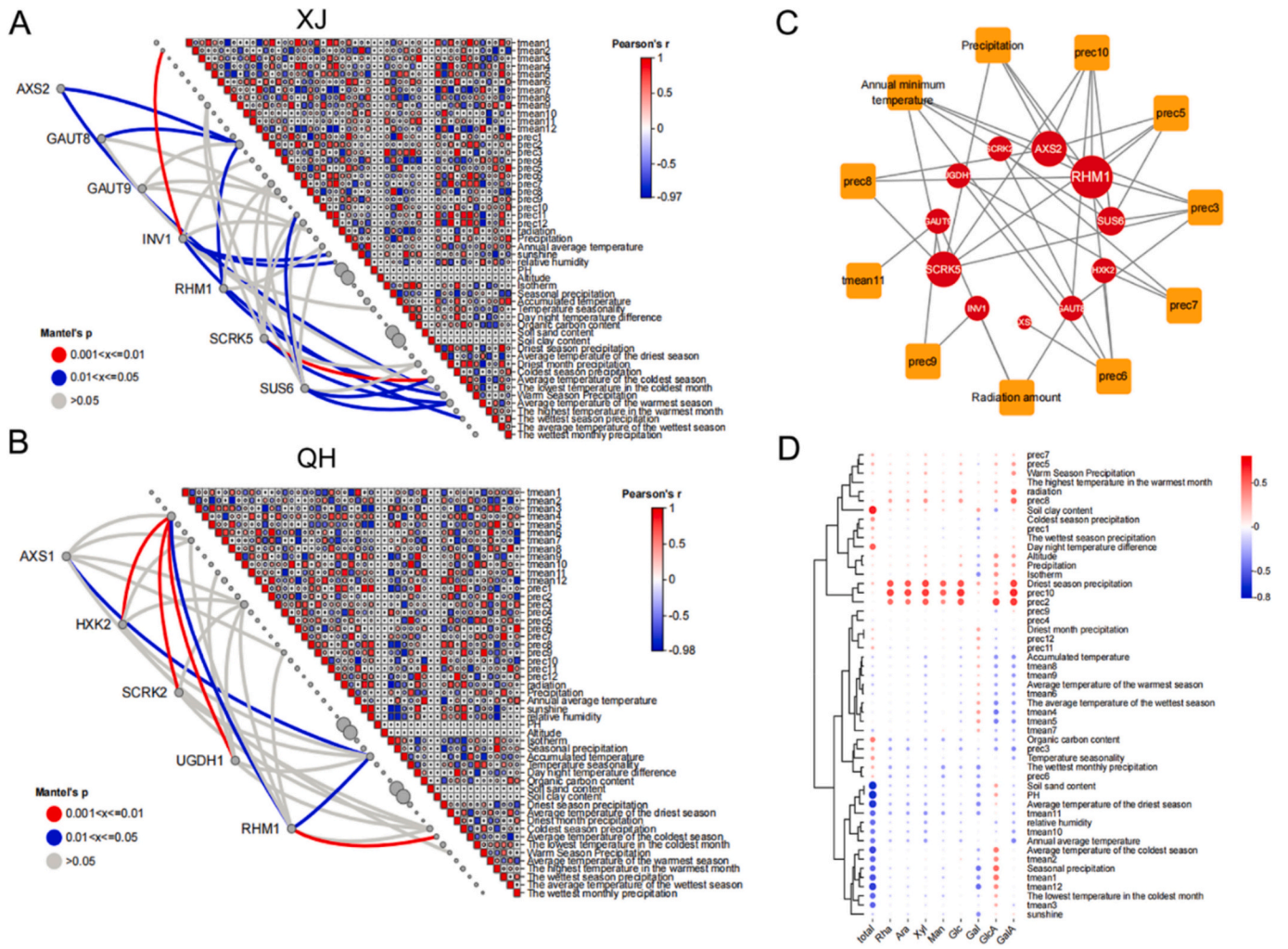

Fig. 7. The effect of environmental factors imposed on DEGs, DEPs and LFPs structures. (A) Mantel test of polysaccharide genes and environmental factors in NX vs XJ. (B) Mantel test of polysaccharide genes and environmental factors in NX vs QH. (C)The network diagram of genes and environmental factors with a correlation greater than 0.5 in the Mantel test. (D) Heat map of correlation between polysaccharide content, monosaccharide components, and environmental factors.

pathway of LFPs was significantly influenced by environmental factors, ultimately impacting the chemical structure of LFPs.

These findings elucidated the biosynthetic mechanism of L. fructus polysaccharides and provided a scientific foundation for the further elucidation of physical processing suitability. However, some critical questions remain open. One concerns the multiple components of polysaccharides to maintain cell wall integrity. Only soluble LFPs were focused in the current research. Actually, a significant quantity of cellulose, diverse hemicellulose, and structurally flexible pectin components collaborate to uphold the integrity of the cell wall. These intricate polysaccharide constituents respond to alterations in the external environment and stressors. Consequently, they inevitably entail more complex structural modifications, proportional regulation, as well as regulatory mechanisms at both gene and protein levels. All these aspects necessitate further comprehensive investigation in subsequent stages. Another challenge lies within deciphering the exact biosynthesis pathway and key point of LFPs. Despite the interpretative constraints, the efforts of the current work highlighted the participation of LFPs in response to the changing external environment. Additionally, the current study demonstrated the diversity of LFPs structures, which can be comprehensively combined with the results of our previous results on small molecule differences, and provide references for the rational layout and differential development of L. *barbarum* L. resources.

Supplementary data to this article can be found online at https://doi.org/10.1016/j.fochms.2024.100232.

CRediT authorship contribution statement

Limei Tong: Writing – review & editing, Writing – original draft, Formal analysis, Data curation. **Yinxiu Jiang:** Writing – review & editing, Writing – original draft, Visualization, Formal analysis, Data curation. **Xinrun Zhang:** Visualization, Formal analysis, Data curation. **Xia Zhang:** Writing – review & editing, Project administration, Methodology, Funding acquisition. **Yihao Zheng:** Formal analysis, Data curation. **Qiheng Zhao:** Visualization, Formal analysis, Data curation. **Sheng Yu:** Visualization, Formal analysis. **Wenhua Zhang:** Data curation. **Gang Ren:** Data curation. **Zhanping Chen:** Data curation. **Yuling Zhao:** Data curation. **Sheng Guo:** Writing – review & editing, Methodology, Formal analysis, Data curation. **Hui Yan:** Visualization, Methodology, Data curation. **Shulan Su:** Resources. **Yang Pan:** Resources, Project administration. **Jin-ao Duan:** Project administration, Methodology, Funding acquisition. **Fang Zhang:** Writing – review & editing, Writing – original draft, Project administration, Methodology, Funding acquisition.

Declaration of competing interest

The authors declare that they have no known competing financial

interests or personal relationships that could have appeared to influence the work reported in this paper.

Data availability

Data will be made available on request.

Acknowledgments

Supports from the National Natural Science Foundation of China (82474027, 82460767 & U21A20408), Key R&D Programs of Ningxia Hui Autonomous Region (2024BEE03007), and high-level key discipline construction project of the National Administration of Traditional Chinese Medicine-Resource Chemistry of Chinese Medicinal Materials (No. zyyzdxk-2023083) are acknowledged. Mr. Weiran Cao at Xi-an Jiaotong-Liverpool University was acknowledged for his enthusiastic help in English language editing.

References

Barratt, L. J., Franco Ortega, S., & Harper, A. L. (2023). Identification of candidate regulators of the response to early heat stress in climate-adapted wheat landraces via transcriptomic and co-expression network analyses. *Frontiers in Plant Science, 14*, 1–16.

Chen, D., Guo, S., Youyuan, L., Zebin, W., Fang, Z., Dawei, Q., … Jin-ao, D. (2020). Application of electronic tongue in identification of goji from different production regions. *Journal Nanjing University of Chinese Medicine, 36*(5), 615–622.

Chen, X., Guo, S., Wang, J., Li, J., Ni, L., Kang, H., … Duan, J. (2024). Comparison on effects of Lycii Fructus from different origins on $NaIO_3$-induced retinal degenerative diseases in mice by multivariate statistical analysis. *China Journal of Chinese Materia Medica, 49*(16), 4521–4531.

Chen, X., Wei, D., Lin, M., Wang, X., Kang, H., Ni, L., Qian, D., Guo, S., & Duan, J. (2024). Comparative evaluation of four Lycium barbarum cultivars on $NaIO_3$-induced retinal degeneration mice via multivariate statistical analysis. *Journal of Ethnopharmacology, 325*, Article 117889.

Chen, Z., Zhu, B., Peng, X., Li, S., & Zhao, J. (2022). Quality evaluation of *Ophiopogon japonicus* from two authentic geographical origins in China based on physicochemical and pharmacological properties of their polysaccharides. *Biomolecules, 12*(10), 1–17.

Ebert, B., Birdseye, D., Liwanag, A. J. M., Laursen, T., Rennie, E. A., Guo, X., … Scheller, H. V. (2019). The three members of the Arabidopsis glycosyltransferase family 92 are functional B-1,4-galactan synthases. *Plant and Cell Physiology, 59*(12), 2624–2636.

Gericke, M., Amaral, A. J. R., Budtova, T., De Wever, P., Groth, T., Heinze, T., … Fardim, P. (2024). The European polysaccharide network of excellence (EPNOE) research roadmap 2040: Advanced strategies for exploiting the vast potential of polysaccharides as renewable bioresources. *Carbohydrate Polymers, 326*, Article 121633.

Gigli-Bisceglia, N., van Zelm, E., Huo, W., Lamers, J., & Testerink, C. (2022). Arabidopsis root responses to salinity depend on pectin modification and cell wall sensing. *Development (Cambridge), 149*(12), 11–13.

Leszczuk, A., Chylińska, M., Zięba, E., Skrzypek, T., Szczuka, E., & Zdunek, A. (2018). Structural network of arabinogalactan proteins (AGPs) and pectins in apple fruit during ripening and senescence processes. *Plant Science, 275*, 36–48.

Li, X., Jiang, J., Chen, Z., & Jackson, A. (2021). Transcriptomic, proteomic and Metabolomic analysis of flavonoid biosynthesis during fruit maturation in Rubus chingii Hu. *Frontiers in Plant Science, 12*, 1–15.

Liang, X., Liu, M., Yao, A., Cui, W., Wei, Y., Guo, S., Duan, J., Kang, H., Zhou, X., Su, S., Jin, H., Zhang, F., Duan, J., & ao.. (2024). In vitro fermentation characteristics and interaction of neutral and acidic polysaccharides from Lycii fructus on human gut microbiota. *Food Hydrocolloids, 152*, Article 109940.

Lu, Y., Guo, S., Zhang, F., Yan, H., Qian, D. W., Wang, H. Q., … Duan, J. A. (2019). Comparison of functional components and antioxidant activity of *lycium barbarum* L. Fruits from different regions in China. *Molecules, 24*(12), 2228.

Ma, R., Zhang, M., Yang, X., Guo, J., & Fan, Y. (2023). Transcriptome analysis reveals genes related to the synthesis and metabolism of cell wall polysaccharides in goji berry (*Lycium barbarum* L.) from various regions. *Journal of the Science of Food and Agriculture, 103*(14), 7050–7060.

Rial-Hermida, M. I., Rey-Rico, A., Blanco-Fernandez, B., Carballo-Pedrares, N., Byrne, E. M., & Mano, J. F. (2021). Recent Progress on Polysaccharide-Based Hydrogels for Controlled Delivery of Therapeutic Biomolecules. *ACS Biomaterials Science and Engineering, 7*(9), 4102–4127.

Takenaka, Y., Kato, K., Ogawa-Ohnishi, M., Tsuruhama, K., Kajiura, H., Yagyu, K., Takeda, A., Takeda, Y., Kunieda, T., Hara-Nishimura, I., Kuroha, T., Nishitani, K., Matsubayashi, Y., & Ishimizu, T. (2019). Pectin RG-I rhamnosyltransferases represent a novel plant-specific glycosyltransferase family. *Nature Plants, 4*, 669–676.

Teka, N., Alminderej, F. M., Souid, G., El-Ghoul, Y., Le Cerf, D., & Majdoub, H. (2022). Characterization of polysaccharides sequentially extracted from Allium roseum leaves and their Hepatoprotective effects against cadmium induced toxicity in mouse liver. *Antioxidants, 11*(10), 1866.

Vaahtera, L., Schulz, J., & Hamann, T. (2019). Cell wall integrity maintenance during plant development and interaction with the environment. *Nature Plants, 5*, 924–932.

Verbančič, J., Lunn, J. E., Stitt, M., & Persson, S. (2018). Carbon supply and the regulation of Cell Wall synthesis. *Molecular Plant, 11*(1), 75–94.

Wang, C., Peng, D., Zhu, J., Zhao, D., Shi, Y., Zhang, S., Ma, K., Wu, J., & Huang, L. (2019). Transcriptome analysis of Polygonatum cyrtonema Hua: Identification of genes involved in polysaccharide biosynthesis. *Plant Methods, 15*, 65.

Wang, J., Li, S., Zhang, H., & Zhang, X. (2024). A review of *Lycium barbarum* polysaccharides: Extraction, purification, structural-property relationships, and bioactive molecular mechanisms. *Carbohydrate Research, 544*, Article 109230.

Wang, X., Zhang, L., Wu, J., Xu, W., Wang, X., & Lü, X. (2017). Improvement of simultaneous determination of neutral monosaccharides and uronic acids by gas chromatography. *Food Chemistry, 220*, 198–207.

Yuan, Y., Imtiaz, M., Rizwan, M., Dai, Z., Hossain, M. M., Zhang, Y., … Tu, S. (2022). The role and its transcriptome mechanisms of cell wall polysaccharides in vanadium detoxication of rice. *Journal of Hazardous Materials, 425*, Article 127966.

Zhang, C., Kim, E., Cui, J., Wang, Y., Lee, Y., & Zhang, G. (2022). Influence of the ecological environment on the structural characteristics and bioactivities of polysaccharides from alfalfa (*Medicago sativa* L.). *Food & Function, 13*(13), 7029–7045.

Zhang, F., Zhang, X., Guo, S., Cao, F., Zhang, X., Wang, Y., Liu, J., Qian, B., Yan, Y., Chen, P., Xu, C., Liu, C., Qian, D., Duan, J., & ao.. (2020). An acidic heteropolysaccharide from Lycii fructus: Purification, characterization, neurotrophic and neuroprotective activities in vitro. *Carbohydrate Polymers, 249*, Article 116894.

Zhang, F., Zhang, X., Liang, X., Wu, K., Cao, Y., Ma, T., … Duan, J. A. (2022). Defensing against oxidative stress in *Caenorhabditis elegans* of a polysaccharide LFP-05S from Lycii fructus. *Carbohydrate Polymers, 289*, Article 119433.

Zhang, K., Sun, Y., Li, M., & Long, R. (2021). CrUGT87A1, a UDP-sugar glycosyltransferases (UGTs) gene from Carex rigescens, increases salt tolerance by accumulating flavonoids for antioxidation in *Arabidopsis thaliana*. *Plant Physiology and Biochemistry, 159*, 28–36.

Zhang, R., Zhang, Z., Yan, C., Chen, Z., Li, X., Zeng, B., & Hu, B. (2024). Comparative physiological, biochemical, metabolomic, and transcriptomic analyses reveal the formation mechanism of heartwood for *Acacia melanoxylon*. *BMC Plant Biology, 24*(1), 1–21.

Zhang, X., Luo, Y., Wei, G., Li, Y., Huang, Y., Huang, J., … Du, S. (2019). Physicochemical and antioxidant properties of the degradations of polysaccharides from Dendrobium officinale and their suitable molecular weight range on inducing HeLa cell apoptosis. *Evidence-based Complementary and Alternative Medicine, 2019*, 1–11.